Heliyon 8 (2022) e10343

Contents lists available at ScienceDirect

Heliyon

journal homepage: www.cell.com/heliyon

Research article

Eigen-solutions and thermal properties of multi-parameter exponential potential

C.A. Onate [a,*], I.B. Okon [b], M.C. Onyeaju [c], E. Omugbe [d], A.D. Antia [b], J.P. Araujo [e], Chen Wen-Li [f]

[a] Department of Physical Sciences, Reedemer's University, Ede, Nigeria
[b] Theoretical Physics Group, Department of Physics, University of Uyo, Nigeria
[c] Department of Physics, University of Port Harcourt, Choba, Nigeria
[d] Department of Physics, Federal University of Petroleum Resources, Effurun, Nigeria
[e] Department of Mathematics, Instituto Federal do Sudeste de Mina Gerais, Juiz de Fora, Brazil
[f] School of Intelligent Science and Information Engineering, Xi'an Peihua University, Xi'an, 710125, China

ARTICLE INFO

Keywords:
Potential model
Eigen-solutions
Thermodynamic properties
Schrödinger equation
Supersymmetric quantum mechanics approach

ABSTRACT

In this work, we determined an approximate eigen solutions of Modified multi-parameter exponential potential using supersymmetric quantum mechanics approach (SUSY) with improved Greene-Aldrich approximation to the centrifugal term. The energy equation and its corresponding normalised radial wave function were fully obtained. The proposed potential reduces to other useful potentials like Rosen-Morse, Hellmann, Yukawa and Coulomb potential as special cases. The thermodynamic properties like the vibrational mean energy ($U(\beta, V)$), Vibrational heat capacity ($C(\beta, V)$), vibrational entropy ($S(\beta, V)$) and vibrational free energy ($F(\beta, V)$) of the interacting potential were studied via partition function ($Z(\beta, V)$) obtained from the resulting energy equation. This study was applied to three diatomic molecules: Chromium hydride (CrH), Titanium Hydride (TiH) and Thiocynate (ScN). To ascertain the high degree of our analytical mathematical accuracy, we compared the results of special cases with an existing results. These were found to be in excellent agreement with the existing results.

1. Introduction

Because of their numerous applications in chemical, physical, and molecular spectroscopy, many diatomic molecular potentials have been used to study bound state solutions of both relativistic and non-relativistic wave equations. Meanwhile, a thorough understanding of molecular structure is dependent on the atom's inter-nuclear interactions and the molecular potential model under consideration [1]. The Deng-Fan potential [2], Tietz-Wei potential model [3], Improved deformed four parameter exponential potential [4], Tietz-Hua potential [5, 6, 7], Morse and Modified Morse potential [8], Deng-Fan-Eckart potential [9], Molecular attractive potential model [1], Mobius square plus Screened Kratzer potential [10], Four parameter potential [11], Varshni potential [12, 13], New generalized Morse-like potential exists in various forms in all of these potential models. The various forms of the Morse potential, on the other hand, have been used to investigate the physical behavior of semiconductor surfaces and interfaces [14, 15, 16]. The Morse potential has been successfully used to model hydrogen bonds connecting two bases in a pair in the study of thermal denaturation of double DNA, stranded-DNA chains [16, 19, 20, 21, 22]. Morse potential is a better diatomic potential model for describing potential energy than other diatomic potential models. A great deal of research has been done on Morse and other exponential-type potentials. Pena et al. [23], for example, investigated the D-dimensional Schrödinger equation for a class of multi-parameter exponential type potentials, they obtained eigenfunctions and eigenvalues for Mie-Type, Coulomb, and Kratzer-Fues potentials as special cases. Okorie et al. [24] investigated the thermodynamic properties of the improved deformed exponential-type potential (IDEP) for some diatomic systems, they obtained the ro-vibrational energy spectra of the potential model using coordinate transformation and the Greene-Aldrich approximation to centrifugal term. Omugbe et al. [11] investigated the unified treatment of non-relativistic bound state solutions, thermodynamic properties, and expectation values of exponential type potentials within the framework of the semi-classical WKB approach. On a general ground several studies have been reported on the Schrödinger equation for some potentials [25, 26, 27, 28]. The rotational Morse potential as a function of bond length was calculated by Theaban and Wadi [29]. The electronic state of the lithium molecule was

* Corresponding author.
E-mail address: oaclems14@physicist.net (C.A. Onate).

https://doi.org/10.1016/j.heliyon.2022.e10343
Received 25 December 2021; Received in revised form 4 February 2022; Accepted 12 August 2022

Table 1. Spectroscopic constants for the selected diatomic molecules.

Molecules	$D_e(eV)$	$r_e(A^0)$	$\lambda\left(\frac{1}{A^0}\right)$	$\mu(amu)$
CrH	2.13	1.694	1.52179	0.988976
TiH	2.05	1.781	1.32408	0.987371
ScN	4.56	1.768	1.50680	10.628771

Table 2. Bound state energies for CrH, TiH and ScN diatomic molecules for the multi-parameter exponential potential for $(a, a_1, ..a_6 = 1.0)$.

n	l	$E_{nl}(eV)$ CrH	$E_{nl}(eV)$ TiH	$E_{nl}(eV)$ ScN
0	0	-5.936194219	-6.219344374	4.567928358
1	0	-67.71577027	-64.57331478	0.437525808
	1	-32.98985462	-38.66887002	8.349496658
2	0	-169.7832712	-159.0445144	-11.28280451
	1	-151.4127864	-149.6230943	-4.300364506
	2	-124.8431562	-137.2443523	9.329232176
3	0	-302.9326768	-282.2731371	-29.44001840
	1	-297.2199229	-286.1953201	-23.24638829
	2	-288.6291116	-291.6170716	-11.14053317
	3	-279.6634650	-296.8925735	6.347734306
4	0	-463.7828317	-431.9104730	-53.17747594
	1	-468.9688138	-447.7872094	-47.66381268
	2	-476.9766516	-470.4755669	-36.87434564
	3	-485.6139478	-493.4153334	-21.25788804
	4	-493.7892582	-514.2287760	-1.426098604
5	0	-650.8552649	-607.0190157	-81.84799625
	1	-665.9994759	-634.1432880	-76.92886133
	2	-689.8294853	-673.8104132	-67.29273926
	3	-716.1542226	-715.0287443	-53.32180773
	4	-741.6825926	-753.4209217	-35.53861045
	5	-5.936194219	-787.8341849	-14.55649007

Table 3. Bound state energies $-E_{nl}(eV)$ for CrH, TiH and ScN diatomic molecules for the multi-parameter exponential potential for $(a, a_1, ..a_6 = -1.0)$.

n	ℓ	CrH	TiH	ScN
0	0	14.76561920	14.99700294	4.494729246
1	0	94.93805117	85.95508663	14.49676826
	1	47.67966134	71.42467103	4.941165272
2	0	184.5554467	156.3367642	33.78369838
	1	173.5364015	158.2822244	24.77723181
	2	325.2090091	263.5274741	6.277293597
3	0	273.2786336	233.8314015	61.05674970
	1	266.7289626	228.8045777	52.79665123
	2	334.8811815	325.5131118	35.87261603
	3	456.6289312	405.6469371	9.427552545
4	0	374.4338653	331.0250109	94.66432980
	1	365.0324080	319.8787353	87.27384212
	2	387.1866073	431.7608969	72.18171084
	3	563.5410636	546.7204921	48.73505077
	4	656.9335698	620.7096252	15.87341406
5	0	495.9505572	451.8729974	132.8588256
	1	483.2211448	436.8029203	126.3869525
	2	480.7730030	571.4477102	113.2245048
	3	710.7504787	720.4121338	92.92090291
	4	834.6213261	817.5267184	64.76818439
	5	924.9910213	893.7875797	27.76716103

Table 4. Comparison of Eigenvalues $(-E_{nl})$ in atomic units for the Hellmann potential and Coulomb potential.

State	λ	Hellmann			Coulomb		
		Present	NU [39]	PTB [40]	Present	NU [39]	AP [39]
1s	0.001	2.249500	2.250500	2.249000	2.248500	2.248500	2.247001
	0.005	2.247506	2.252506	2.245010	2.242506	2.242506	2.235037
	0.010	2.245025	2.255025	2.240050	2.235025	2.235025	2.220149
2s	0.001	0.562001	0.563001	0.561505	0.561001	0.561001	0.559506
	0.005	0.560025	0.565025	0.557550	0.555025	0.555025	0.547649
	0.010	0.557600	0.567600	0.552697	0.547600	0.547600	0.533091
2p	0.001	0.561250	0.563000	0.561502	0.561750	0.560250	0.559505
	0.005	0.556256	0.565000	0.557541	0.558756	0.551256	0.547624
	0.010	0.550025	0.567500	0.552664	0.555025	0.540025	0.532993
3s	0.001	0.249168	0.250502	0.249004	0.248502	0.248502	0.248502
	0.005	0.245867	0.252556	0.245111	0.242556	0.242556	0.235332
	0.010	0.241803	0.255225	0.240435	0.235225	0.235225	0.221306
3p	0.001	0.249168	0.250501	0.249004	0.248835	0.248168	0.247012
	0.005	0.245867	0.252531	0.245103	0.244201	0.240867	0.235308
	0.010	0.241803	0.255125	0.240404	0.238469	0.231803	0.221212
3d	0.001	0.248500	0.250833	0.249003	0.249500	0.247500	0.247010
	0.005	0.242506	0.254151	0.245086	0.247506	0.237506	0.235259
	0.010	0.235025	0.258269	0.240341	0.245025	0.225025	0.221024

calculated using the effective potential. Sanjib and Debnath [30] investigated Woods-Saxon plus Rosen-Morse potential solutions within the framework of the Nikiforov-Uvarov method. They derived the eigenfunctions and eigenvalues of the Woods-Saxon potential, as well as the PT and non-PT symmetric solutions of the Rosen-Morse potential. Nasser et al. [31] used triadiagonal J-matrix representation to investigate the bound state of the rotating Morse potential model for diatomic systems. For arbitrary angular momentum, they obtained the bound state energy spectrum for some diatomic systems (H2, LiH, HCl, and CO). The asymptotic iteration method was used by Barakat and Abodayeh [32] to investigate the exact solutions for vibrational levels of the Morse potential. In this paper, we use supersymmetric quantum mechanics approach to investigate the bound state solutions of the Schrödinger equation with a modified multiple parameter exponential potential. The energy eigen equation is presented in closed form, and it is extended to study partition function and other thermodynamic properties. This article is broken down into five sections. Section 1 provides a brief overview of the article. Section 2 presents the bound state solution of the proposed potential using a supersymmetric quantum mechanics approach. Section 3 presents the thermodynamic properties of the proposed potential. Section 4 discusses the numerical results, while Section 5 concludes the article.

2. Radial solution of Schrödinger equation using supersymmetric quantum mechanics approach (SUSY)

The bound state solutions for the proposed potential is obtained in this section. The radial Schrödinger equation as

$$-\frac{\hbar^2}{2\mu}\frac{d^2R_{n,\ell}(r)}{dr^2}+V(r)R_{n,\ell}(r)+\frac{\hbar^2}{2\mu}\frac{\ell(\ell+1)}{r^2}R_{n,\ell}(r)=E_{n,\ell}R_{n,\ell}(r), \tag{1}$$

where the energy of the is $E_{n,\ell}$, $\hbar$ is Planck's constant, μ is the reduced mass, $R_{n,\ell}(r)$ is the wave function and $V(r)$ is the interacting potential given by

$$V(r)=D_e\left[a+a_0\lambda+\frac{a_1\lambda+(a_2+a_3\lambda+a_4e^{\lambda r_e})e^{-\lambda r}}{1-e^{-\lambda r}}+\frac{a_5+a_6e^{2\lambda r_e}}{(1-e^{-\lambda r})^2}e^{-2\lambda r}\right]. \tag{2}$$

The centrifugal term in Eq. (1) can be approximated by the formula [33].

$$\frac{1}{r^2}\approx\frac{\lambda^2}{(1-e^{-\lambda r})^2}. \tag{3}$$

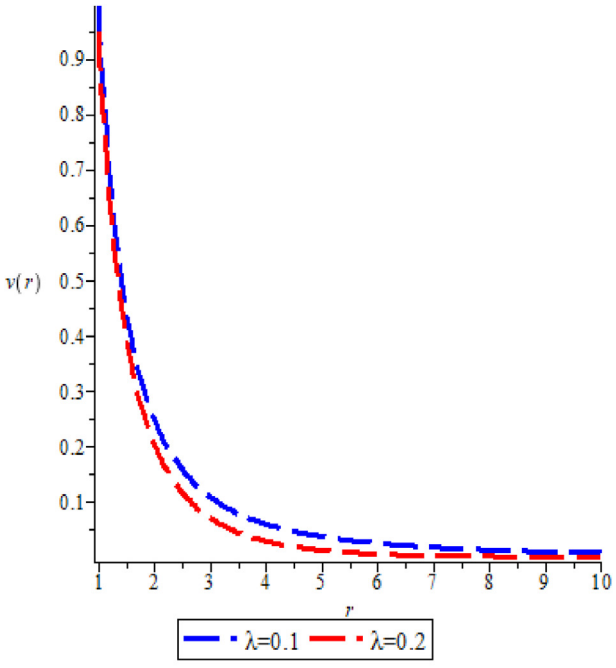

(a)

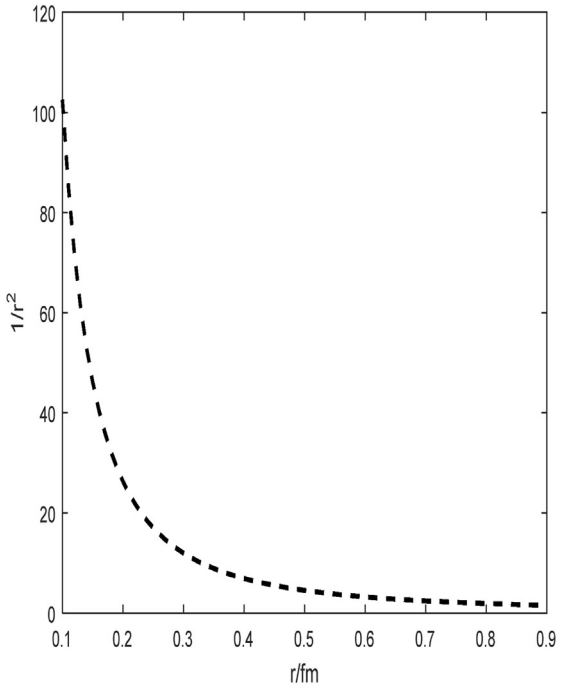

(b)

Figure 1. (a): The variation of multi-parameter exponential potential with the screening parameter. (b): The approximation scheme in Eq. (3).

To solve equation in Eq. (1) using supersymmetric approach, Eq. (2) and Eq. (3) are first substituted into Eq. (1) to have

$$\frac{d^2R_{n,\ell}(r)}{dr^2}=\left[V_P+\frac{\frac{2\mu a_1\lambda D_e}{\hbar^2}+V_Te^{-\lambda r}}{1-e^{-\lambda r}}+\frac{V_Re^{-2\lambda r}-\ell(\ell+1)\lambda^2e^{-\lambda r}}{(1-e^{-\lambda r})^2}\right]R_{n,\ell}(r), \quad (4)$$

where

$$V_P=\ell(\ell+1)\lambda^2+\frac{2\mu(aD_e+a_0\lambda D_e-E_{n,\ell})}{\hbar^2}, \quad (5)$$

$$V_T=\frac{2\mu D_e(a_2+a_3\lambda+a_4e^{\lambda r_e})}{\hbar^2}-\ell(\ell+1)\lambda^2, \quad (6)$$

$$V_R=\frac{2\mu D_e(a_5+a_6e^{2\lambda r_e})}{\hbar^2}. \quad (7)$$

Eq. (5), Eq. (6) and Eq. (7), are used for simplicity. The use of supersymmetric approach involves the proposition of superpotential function as a general solution to Riccati equation. Thereafter, the supersymmetric partner potential can be constructed where a simple mapping of the desire result is formed to determine the energy equation [34, 35, 36]. To proceed from Eq. (4), first the ground state wave function is written as

$$R_{0,\ell}(r)=exp\left(-\int W(r)dr\right), \quad (8)$$

Where $W(r)$ is called superpotential function in supersymmetric quantum mechanics. The ground state wave function corresponds to the two partner Hamiltonians [37].

$$H_+=\widehat{A}\widehat{A}^\dagger=-\frac{d^2}{dr^2}+V_+(r), \quad (9)$$

$$H_-=\widehat{A}^\dagger\widehat{A}=-\frac{d^2}{dr^2}+V_-(r), \quad (10)$$

where

$$\widehat{A}^\dagger=-\frac{d}{dr}-W(r), \quad (11)$$

$$\widehat{A}=\frac{d}{dr}-W(r). \quad (12)$$

Substituting Eq. (8) into Eq. (4) leads to a non-linear Riccati equation of the form

$$W^2(r)-\frac{dW(r)}{dr}=V_P+\frac{\frac{2\mu a_1\lambda D_e}{\hbar^2}+V_Te^{-\lambda r}}{1-e^{-\lambda r}}+\frac{V_Re^{-2\lambda r}-\ell(\ell+1)\lambda^2e^{-\lambda r}}{(1-e^{-\lambda r})^2}, \quad (13)$$

To proceed from Eq. (13), we propose a superpotential function of the form

$$W(r)=\rho_0+\frac{\rho_1}{1-e^{-\lambda r}}, \quad (14)$$

and substituting it into Eq. (13) with the consideration that the radial wave equation satisfy the boundary conditions that $R_{n,\ell}(r)/r$ becomes zero as $r\to\infty$, and $R_{n,\ell}(r)/r$ is finite when $r=0$, some simple mathematical manipulations and simplifications result to the following equations

$$\rho_0^2=V_P \quad (15)$$

$$\rho_1=\frac{\lambda\pm\sqrt{\lambda^2+4\ell(\ell+1)\lambda^2+4V_R\lambda^{-2}}}{2}, \quad (16)$$

$$\rho_0=\frac{V_R+V_T-\frac{2\mu a_1\lambda D_e}{\hbar^2}}{2\rho_1}-\frac{\rho_1}{2}. \quad (17)$$

Eq. (15), Eq. (16) and Eq. (17) are the bases for the energy equation. Using Eq. (14) in conjunction with Eqs. (9), (10), (11), and (12), the two partner potentials of the supersymmetry quantum mechanics can fully be written in the form

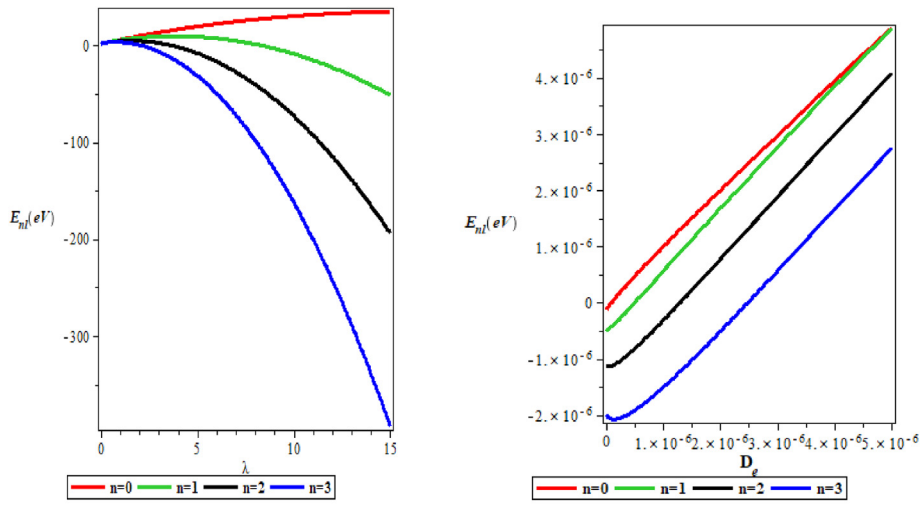

(a) (b)

Figure 2. Variation of bound state energy spectral with screening parameter λ (a) and dissociation energy D_e (b).

$$V_+(r) = W^2(r) + \frac{dW(r)}{dr} = \rho_0^2 + \frac{\rho_1(2\rho_0+\lambda)}{1-e^{-\lambda r}} + \frac{\rho_1(\rho_1-\lambda)}{(1-e^{-\lambda r})^2}, \tag{18}$$

$$V_-(r) = W^2(r) - \frac{dW(r)}{dr} = \rho_0^2 + \frac{\rho_1(2\rho_0-\lambda)}{1-e^{-\lambda r}} + \frac{\rho_1(\rho_1+\lambda)}{(1-e^{-\lambda r})^2}. \tag{19}$$

It can be seen from Eq. (18) and Eq. (19) that the family potentials satisfied a shape invariance condition which established a relation of the form

$$V_+(a_0, r) = V_-(a_1, r) + R(a_1), \tag{20}$$

via mapping of the form $\rho_1 \to \rho_1 + \lambda$, where $\rho_1 = a_0$. In terms of the parameters of the partner potentials in Eq. (20), the relation $a_1 = f(a_0) = a_0 + n$, where a_1 is a new set of parameters uniquely determined from an old set of parameters a_0, the term $R(a_1)$, is called a remainder or residual term and it is independent of the variable r. Since $a_1 = a_0 + \lambda$, then, $a_2 = a_0 + 2\lambda$, $a_3 = a_0 + 3\lambda$, $a_4 = a_0 + 4\lambda$, subsequently, the recurrence relation is generalized as $a_n = a_0 + n\lambda$. Using the shape invariance approach [37], the recurrence relations above, Eq. (20) is transformed as

$$R(a_1) = \left(\frac{V_R + V_T - \frac{2\mu a_1 \lambda D_e}{\hbar^2} - a_0^2}{2a_0}\right)^2 - \left(\frac{V_R + V_T - \frac{2\mu a_1 \lambda D_e}{\hbar^2} - a_1^2}{2a_1}\right)^2, \tag{21}$$

$$R(a_2) = \left(\frac{V_R + V_T - \frac{2\mu a_1 \lambda D_e}{\hbar^2} - a_1^2}{2a_1}\right)^2 - \left(\frac{V_R + V_T - \frac{2\mu a_1 \lambda D_e}{\hbar^2} - a_2^2}{2a_2}\right)^2, \tag{22}$$

$$R(a_3) = \left(\frac{V_R + V_T - \frac{2\mu a_1 \lambda D_e}{\hbar^2} - a_2^2}{2a_2}\right)^2 - \left(\frac{V_R + V_T - \frac{2\mu a_1 \lambda D_e}{\hbar^2} - a_3^2}{2a_3}\right)^2, \tag{23}$$

$$R(a_n) = \left(\frac{V_R + V_T - \frac{2\mu a_1 \lambda D_e}{\hbar^2} - a_{n-1}^2}{2a_{n-1}}\right)^2 - \left(\frac{V_R + V_T - \frac{2\mu a_1 \lambda D_e}{\hbar^2} - a_n^2}{2a_n}\right)^2, \tag{24}$$

Using the negative partner potential, the energy equation of the system can be written as

$$E_{n\ell} = \sum_{k=1}^{v} R(a_k) = -\left(\frac{V_R + V_T - \frac{2\mu a_1 \lambda D_e}{\hbar^2} - a_n^2}{2a_n}\right)^2, \tag{25}$$

which on correct substitution of the parameters of the system into Eq. (25) using Eqs. (15), (16), and (17) and Eqs. (21), (22), (23), and (24) gives a complete energy equation in a one-dimensional system as

$$E_{n\ell} = D_e\left(a + a_0\lambda + a_1\lambda\right) + \frac{\lambda^2\hbar^2}{2\mu}\left[\ell\left(\ell+1\right) - \left(\frac{\frac{2\mu D_e(\beta_0+\beta_1)}{\lambda^2\hbar^2} - \ell\left(\ell+1\right)}{2n+1+\delta_0} - \frac{2n+1+\delta_0}{4}\right)^2\right]. \tag{26}$$

$$\delta_0 = \sqrt{(1+2\ell)^2 + \frac{8\mu D_e(a_5 + a_6 e^{2\lambda r_e})}{\lambda^2\hbar^2}} \tag{27}$$

$$\beta_0 = a_2 + a_5 + \lambda(a_3 - a_1) \tag{28}$$

$$\beta_1 = e^{\alpha r_e}\left(a_4 + a_6 e^{\lambda r_e}\right) \tag{29}$$

where Eq. (27), Eq. (28) and Eq. (29) are used for simplicity.

2.1. Special cases

The proposed potential model given in Eq. (2) can be reduced to some potential models by varying the potential parameters.

(a) *Improved Rosen-Morse-like Potential* [38].

Substituting $a_0 = a_1 = a_3 = 0$, into Eq. (26) gives the energy of Improved Rosen-Morse-like potential as

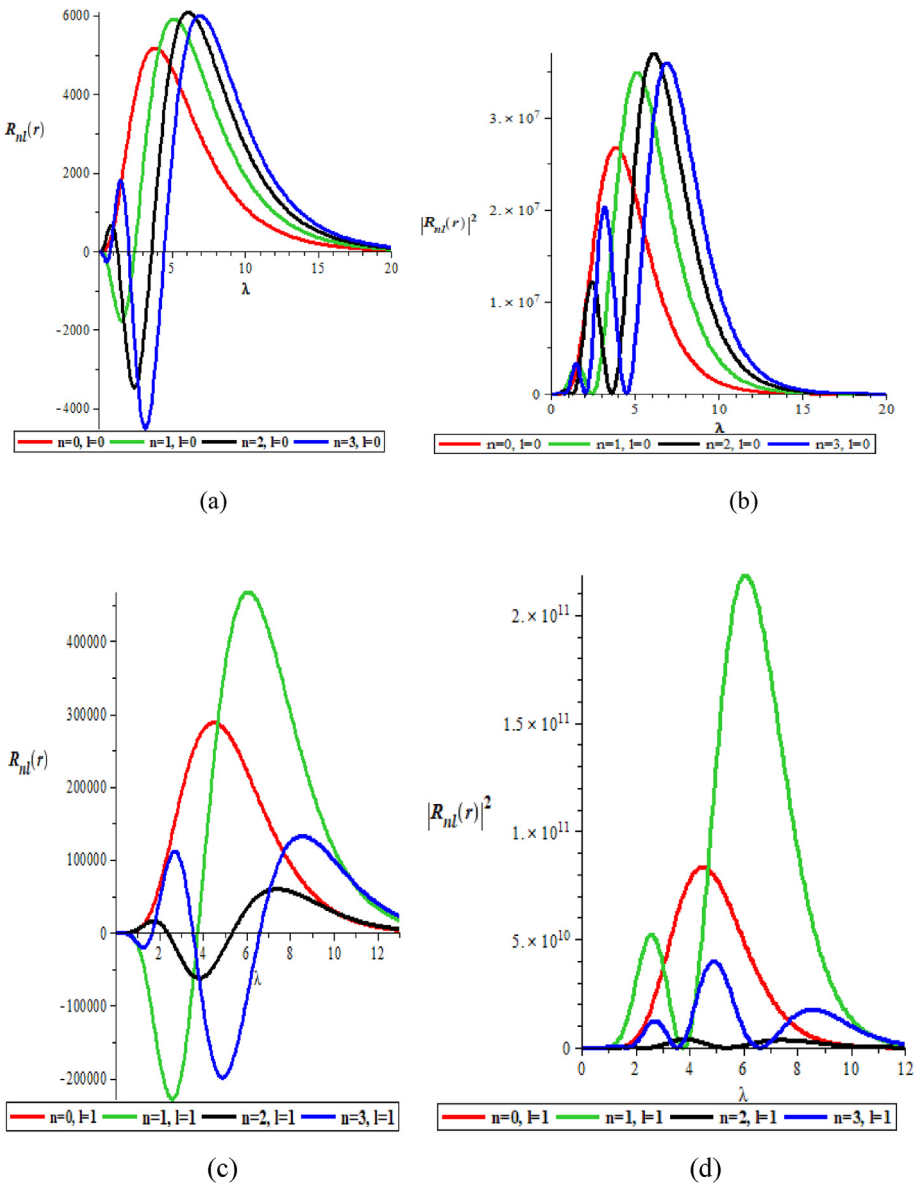

Figure 3. Wave function and probability density plots for $l = 0$ (a–b) and $l = 1$ (c–d).

$$E_{n\ell} = D_e a + \frac{\lambda^2\hbar^2}{2\mu}\left[\ell\left(\ell+1\right) - \left(\frac{\frac{2\mu D_e\left(a_2+a_5+a_4e^{2re}+a_6e^{2re}\right)}{\lambda^2\hbar^2} - \ell\left(\ell+1\right)}{2n+1+\delta_0} - \frac{2n+1+\delta_0}{4}\right)^2\right]. \tag{30}$$

(b) *Hellmann Potential.*

Substituting $a = a_0 = a_2 = a_4 = a_5 = a_6 = 0$ into Eq. (26) gives the energy of Hellmann potential as

$$E_{n\ell} = \lambda a_1 D_e + \frac{\lambda^2\hbar^2}{2\mu}\left[\ell\left(\ell+1\right) - \left(\frac{\frac{2\mu D_e(a_3-a_1)}{\lambda\hbar^2} - \ell\left(\ell+1\right) - (1+n+\ell)^2}{2(1+n+\ell)}\right)^2\right]. \tag{31}$$

(c) Yukawa Potential

Substituting $a = a_0 = a_1 = a_2 = a_4 = a_5 = a_6 = 0$ into Eq. (26) gives the energy equation of Yukawa potential as

$$E_{n\ell} = \frac{\ell(\ell+1)\lambda^2\hbar^2}{2\mu}\left[\ell(\ell+1) - \left(\frac{\frac{2\mu D_e a_3}{\lambda\hbar^2} - \ell(\ell+1) - (1+n+\ell)^2}{2(1+n+\ell)}\right)^2\right]. \tag{32}$$

(d) Coulomb Potential

Substituting $a = a_0 = a_2 = a_3 = a_4 = a_5 = a_6 = 0$ into Eq. (26) gives the energy equation of Coulomb potential as

$$E_{n\ell} = \lambda a_0 D_e + \frac{\lambda^2\hbar^2}{2\mu}\left[\ell(\ell+1) - \left(\frac{-\frac{2\mu D_e a_1}{\lambda\hbar^2} - \ell(\ell+1) - (1+n+\ell)^2}{2(1+n+\ell)}\right)^2\right]. \tag{33}$$

Using the constant $a = a_1 = a_2 = a_3 = a_4 = a_5 = a_6 = 0$, Eq. (33) can further be reduced to

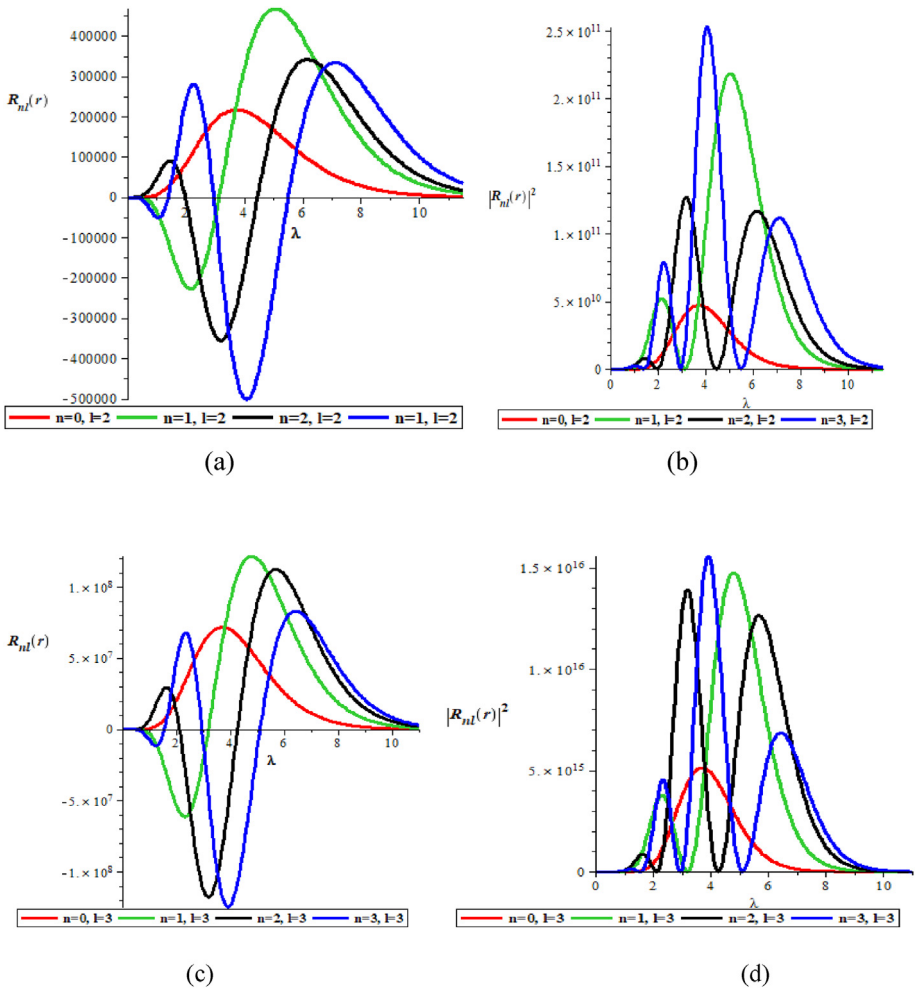

Figure 4. Wave function and probability density plots for $l = 2$ (a–b) and $l = 3$ (c–d).

$$E_{n\ell} = D_e a_0 \lambda + \frac{\lambda^2 \hbar^2}{2\mu}\left[\ell(\ell+1) - D_e\left(\frac{-\ell(\ell+1) - (1+n+\ell)^2}{2(1+n+\ell)}\right)^2\right]. \quad (34)$$

Eq. (30), Eq. (31), Eq. (32), Eq. (33) and Eq. (34) are special cases of Eq. (26). The total wave function for the proposed potential is given as

$$R_{n,\ell}(y) = y^{\beta}(1-y)^{\eta} F_1(-n, n+2(\beta+\eta); 2\beta+1, y), \quad (35)$$

where

$$\beta = \sqrt{\ell(\ell+1) + \frac{2\mu D_e(a + a_0\lambda + a_1\lambda) - 2\mu E_{n,\ell}}{\lambda^2\hbar^2}}, \quad (36)$$

$$\eta = \sqrt{(2\ell+1)^2 + \frac{8\mu D_e(a_5 + a_6 e^{2\lambda r_e})}{\lambda^2\hbar^2}}, \quad (37)$$

and F is the hypergeometric function. Eq. (36) and Eq. (37) are used as simplicity. To obtain the normalization constant of Eq. (35), we employ the normalization condition

$$\int_0^{\infty} |R_{nl}(r)|^2 dr = 1 \Rightarrow \int_0^{\infty} \left[N_{nl} y^{\beta}(1-y)^{\eta} P_n^{(2\beta,2\eta-1)}(1-2y)\right]^2 dy = 1. \quad (38)$$

The wave function is assumed to be in bound at $r \in (0, \infty)$ and $y = e^{-\lambda r} \in (1, 0)$.

Eq. (38) reduces to

$$-\frac{N_{nl}^2}{\lambda}\int_1^0 y^{2\beta}(1-y)^{2\eta}\left[P_n^{(2\beta,2\eta-1)}(1-2y)\right]^2 \frac{dy}{y} = 1 \quad (39)$$

Let $z = (1-2y)$ such that the boundary of integration of Eq. (39) changes from $y \in (1, 0)$ to. $z \in (-1, 1)$. Then Eq. (39) reduces to

$$\frac{N_{nl}^2}{2\lambda}\int_{-1}^{1}\left(\frac{1-z}{2}\right)^{2\beta-1}\left(\frac{1+z}{2}\right)^{2\eta}\left[P_n^{(2\beta,2\eta-1)}(z)\right]^2 dz = 1 \quad (40)$$

Using the standard integral [31]

$$\int_{-1}^{1}\left(\frac{1-w}{2}\right)^{x}\left(\frac{1+w}{2}\right)^{y}\left[P_n^{(x,y-1)}(w)\right]^2 dw = \frac{2^{x+y+1}\Gamma(x+n+1)\Gamma(y+n+1)}{n!\Gamma(x+y+n+1)\Gamma(x+y+2n+1)} \quad (41)$$

where we assume that $z = w$, $x = 2\beta - 1$, $y = 2\eta$. Then, using equation (40) and Eq. (41), the normalization constant can be obtained as

$$N_{nl} = \sqrt{\frac{2\lambda(n!)\Gamma(2\beta+2\eta+n)\Gamma(2\beta+2\eta+2n)}{2^{(2\beta+2\eta)}\Gamma(2\beta+n)\Gamma(2\eta+n+1)}}. \quad (42)$$

Using Eq. (42), the total normalized wave function is given as

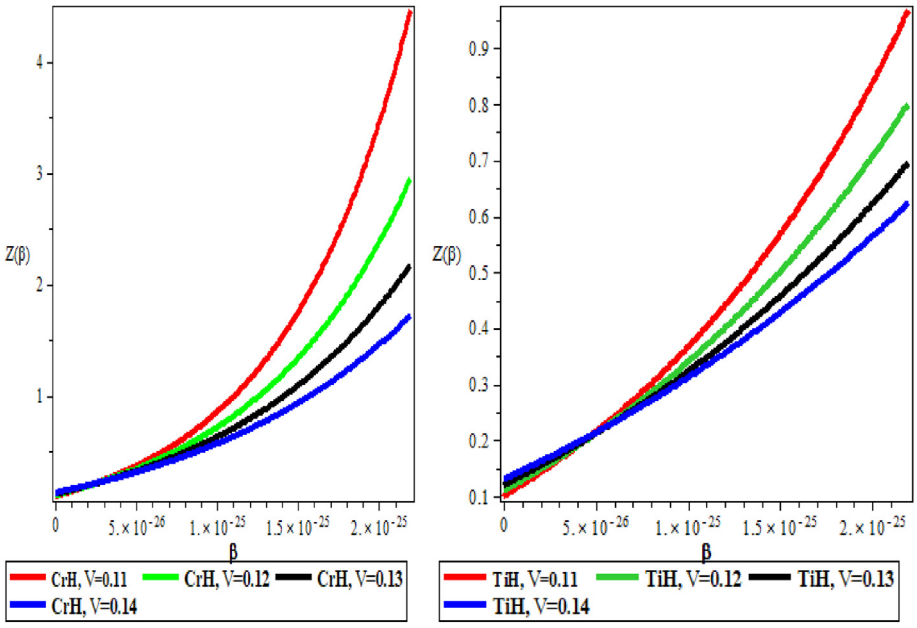

(a) CrH (b) TiH

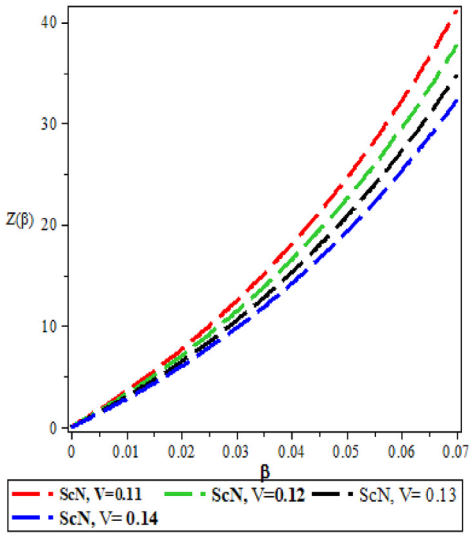

(c) ScN

Figure 5. Variation of Z(β) against β for CrH (a), TiH (b) and ScN (c).

$$\sqrt{\frac{2\lambda(n!)\Gamma(2\beta+2\eta+n)\Gamma(2\beta+2\eta+2n)}{2^{(2\beta+2\eta)}\Gamma(2\beta+n)\Gamma(2\eta+n+1)}}\, y^{\beta}(1-y)^{\eta}P_n^{(2\beta,2\eta-1)}(1-2y) \tag{43}$$

Eq. (43) is a complete normalized radial wave function of the system.

3. Thermodynamic properties for the modified four parameter Morse potential

The thermodynamic properties of quantum systems can be obtained from the exact partition function given by

$$Z(\beta) = \sum_{n=0}^{V} e^{-\beta E_n} \tag{44}$$

where, V is an upper bound of the vibrational quantum number obtained from the numerical solution of $\frac{dE_n}{dn} = 0$, $\beta = \frac{1}{kT}$ where k and T are Boltzmann constant and absolute temperature respectively. In the classical limit, the summation in Eq. (44) can be replaced with an integral:

$$Z(\beta) = \int_0^V e^{-\beta E_n} dn. \tag{45}$$

Eq. (45) is the equation for partition function. The energy Eq. (26) can be simplified further as

$$E_{nl} = \upsilon_1 - \upsilon_2\left[\frac{\upsilon_3}{(n+\delta)} - (n+\delta)\right]^2. \tag{46}$$

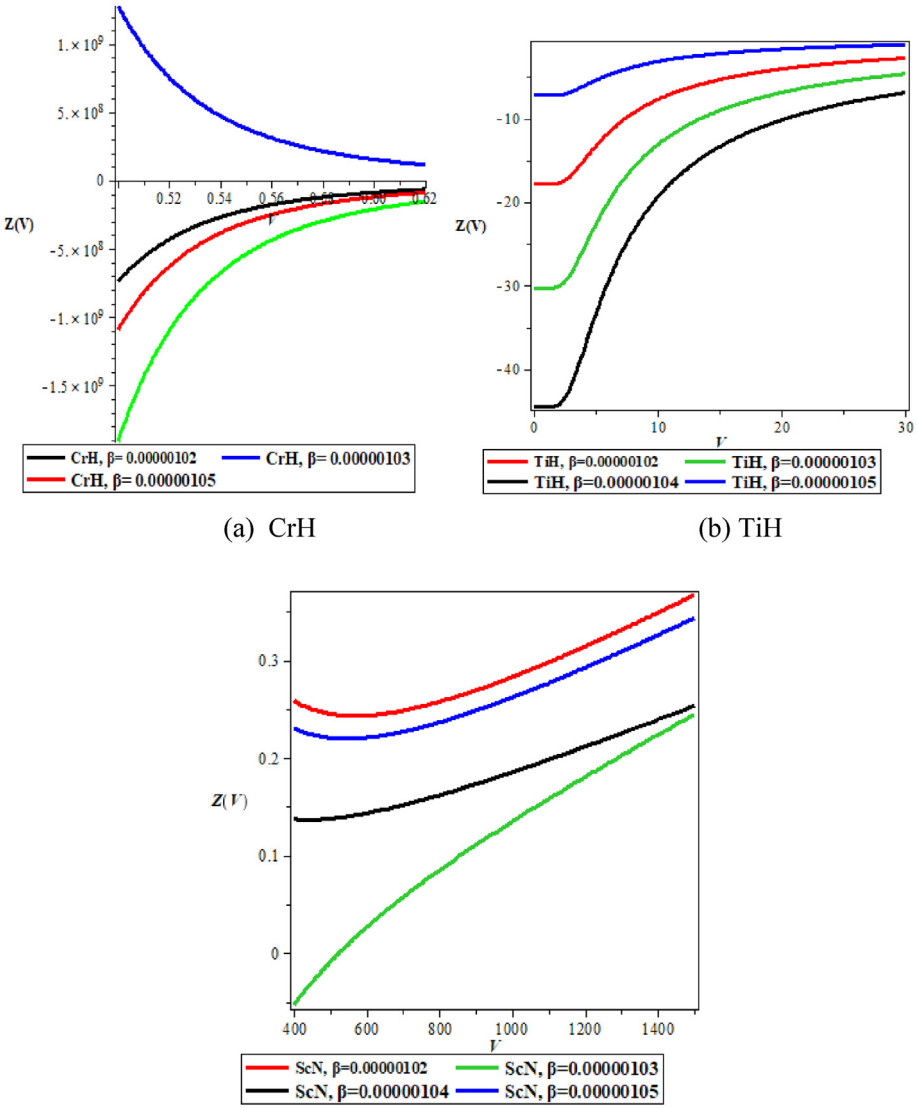

(a) CrH (b) TiH

(c) ScN

Figure 6. Variation of Z(λ) against λ for CrH (a), TiH (b) and ScN (c).

where

$$\left.\begin{aligned} \upsilon_1 &= D_e(a + a_0 + a_1\lambda) + \frac{\hbar^2\lambda^2 l(l+1)}{2\mu}\,; \quad \upsilon_3 = \frac{2\mu D_e(\beta_0+\beta_1)}{\hbar^2\lambda^2} - l(l+1)\,, \\ \upsilon_2 &= \frac{\hbar^2\lambda^2}{8\mu}\,; \quad \delta = \frac{1}{2} + \frac{1}{2}\sqrt{(1+2l)^2 + \frac{8\mu D_e\left(a_5 + a_6 e^{2\lambda r_e}\right)}{\hbar^2\lambda^2}} \end{aligned}\right\}. \tag{47}$$

Let $\rho = (n+\delta)$, then Eq. (46) can then be express as

$$E_{nl} = -\left[\upsilon_2\rho^2 + \frac{\upsilon_2\upsilon_3^2}{\rho^2}\right] + \upsilon_1 - 2\upsilon_2\upsilon_3 \tag{48}$$

Using Eq. (47) and Eq. (48), the partition function of Eq. (26) can then be express as

$$Z(\beta) = e^{\beta(2\upsilon_2\upsilon_3-\upsilon_1)} \int_0^V e^{\beta\left[\upsilon_2\rho^2 + \frac{\upsilon_2\upsilon_3^2}{\rho^2}\right]} d\rho \tag{49}$$

Using Mathematica 10.0 version, the partition function of Eq. (49) is obtained as

$$Z(\beta) = \frac{\left[e^{\chi_1-\chi_2}(1+\chi_4) + e^{\chi_1+\chi_3}(-1+\chi_5)\right]}{4\sqrt{-\beta\upsilon_2}} \tag{50}$$

where

$$\left.\begin{aligned} \chi_1 &= \beta(-\upsilon_1 + 2\upsilon_2\upsilon_3)\,, \ \chi_2 = 2\sqrt{-\beta\upsilon_2}\sqrt{-\beta\upsilon_2\upsilon_3^2}\,, \chi_3 = -2\sqrt{-\beta\upsilon_2}\sqrt{-\beta\upsilon_2\upsilon_3^2}\,, \\ \chi_4 &= erf\left[V\sqrt{-\beta\upsilon_2} - \frac{\sqrt{-\beta\upsilon_2\upsilon_3^2}}{V}\right], \chi_5 = erf\left[\lambda\sqrt{-\beta\upsilon_2} + \frac{\sqrt{-\beta\upsilon_2\upsilon_3^2}}{V}\right] \end{aligned}\right\}. \tag{51}$$

Eq. (50) gives the complete partition function while Eq. (51) is used for simplicity.

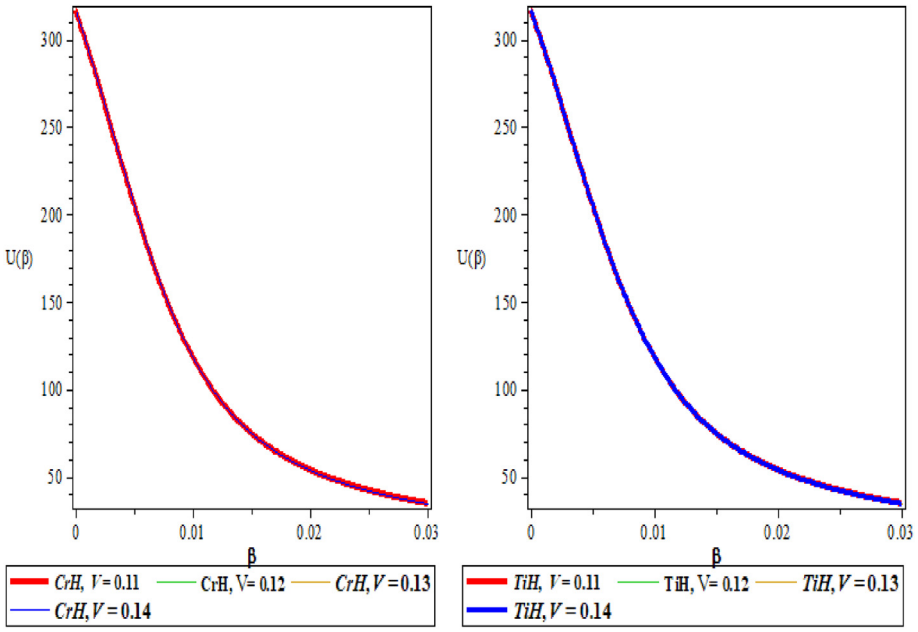

(a) (b)

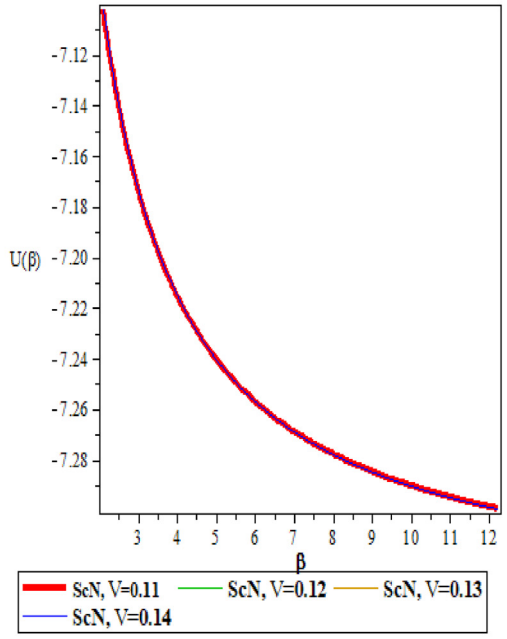

(c)

Figure 7. Variation of U(β) against β for CrH (a), TiH (b) and ScN (c).

(a) Vibrational mean energy

$$U(\beta) = -\frac{\partial \ln Z(\beta)}{\partial \beta} = U(\beta) = -\left\{ \frac{\left[\begin{array}{l} 1+\chi_4+e^{2\chi_2}(\chi_5-1)-2\beta\left[1+\chi_4+e^{2\chi_2}(\chi_5-1)\right]\omega_0+ \\ \omega_1 4\sqrt{-\beta\upsilon_2}\left[\sqrt{\pi}\beta\left(-1-e^{2\chi_2}-\chi_4+e^{2\chi_2}\chi_5\right)\upsilon_2\upsilon_3^2-e^{\chi_2+w_2}\right] \end{array} \right]}{2\beta\left[1+\chi_4+e^{2\chi_2}(-1+\chi_5)\right]} \right\}. \quad (52)$$

where

$$w_0 = (-\upsilon_1+2\upsilon_2\upsilon_3),\ w_1 = \frac{1}{\sqrt{\pi}\sqrt{-\beta\upsilon_2\upsilon_3^2}},\ w_2 = \frac{\beta\upsilon_2\left(\lambda^4+\upsilon_3^2\right)}{\lambda^2}\lambda\sqrt{-\beta\upsilon_2\upsilon_3^2}\Big\}. \quad (53)$$

Eq. (52) is a vibrational mean energy while Eq. (53) are used for simplicity.

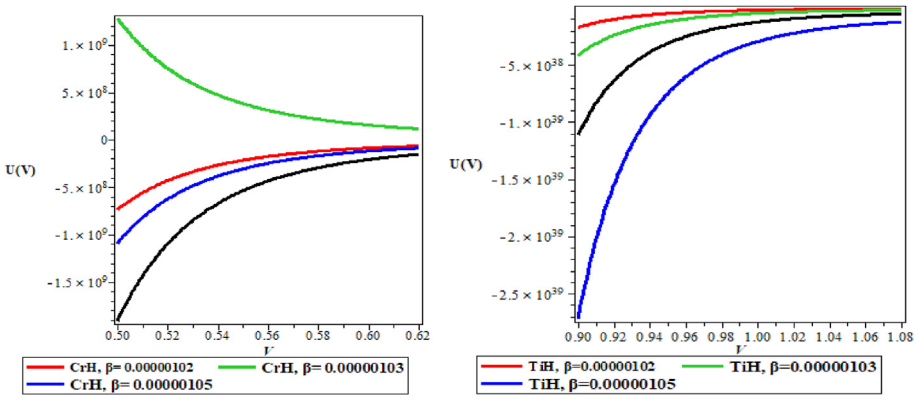

(a) (b)

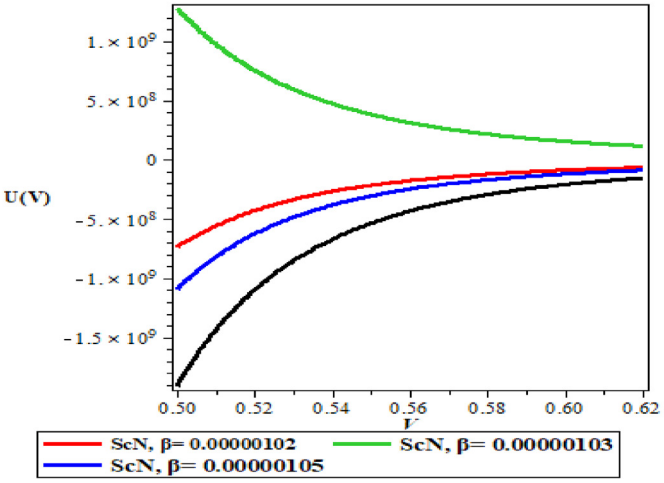

(c)

Figure 8. Variation of U(λ) against λ for CrH (a), TiH (b) and ScN (c).

(b) Vibrational Specific heat capacity

$$C(\beta)=K\beta^2\frac{\partial^2 InZ(\beta)}{\partial\beta^2}$$
$$=\left\{\frac{\left[\pi\lambda(1-e^{2\chi_2}+\chi_4+e^{2\chi_2}\chi_5)^2\omega_3+\Phi_0+\Phi_1+\Phi_2-8e^{\chi_2}\sqrt{\pi}\lambda\omega_3+\Phi_3+\chi_4\Phi_4\right]}{\left[2\pi\lambda(1-e^{2\chi_2}+\chi_4+e^{2\chi_2}\chi_5)^2\omega_3\right]}\right\} \quad (54)$$

where

Eq. (54) is a vibrational specific heat capacity while Eq. (55) is used for simplicity.

$$\left.\begin{aligned}
&\Phi_0=2e^{\chi_2+\omega_2}\beta\lambda^2\upsilon_2\left[\begin{matrix}\sqrt{\pi}-e^{2\chi_2}\sqrt{\pi}+\sqrt{\pi}\chi_4\\+e^{2\chi_2}\sqrt{\pi}\chi_5+4e^{\chi_2+\omega_2}\lambda\sqrt{-\beta\upsilon_2}\end{matrix}\right]\omega_6,\Phi_1=4e^{\chi_2}\sqrt{\pi}\beta^2\upsilon_2^2\left[-e^{\omega_4}\lambda^4\left(1-e^{2\chi_2}+\chi_4+e^{2\chi_2}\chi_5\right)\right]\omega_6,\\
&\Phi_2\upsilon_3^2\left(4e^{\omega_2}\omega_5+4e^{2\chi_2+\omega_2}\omega_5+e^{\omega_2}\omega_6-e^{2\chi_2+\omega_2}\omega_6\right),\Phi_3=e^{\chi_2}\chi_5\left[8\sqrt{\pi}\lambda\omega_3+e^{\chi_2+\omega_2}\left(-4\lambda^2\sqrt{-\beta\upsilon_2}+\sqrt{-\beta\upsilon_2\upsilon_3^2}\right)\right],\\
&\Phi_4=\left[-8e^{\chi_2}\sqrt{\pi}V\Lambda_3+8e^{\chi_2}\sqrt{\pi}V\omega_3+e^{\Lambda_2}\left(4V^2\omega_3\right)\right],\omega_3=\sqrt{-\beta\upsilon_2}\sqrt{-\beta\upsilon_2\upsilon_3^2},\omega_4=\frac{\beta\upsilon_2\left(V^4+\upsilon_3^2\right)}{V^2},\\
&\omega_5=V^2\sqrt{-\beta\upsilon_2},\ \omega_6=\sqrt{-\beta\upsilon_2\upsilon_3^2}
\end{aligned}\right\} \quad (55)$$

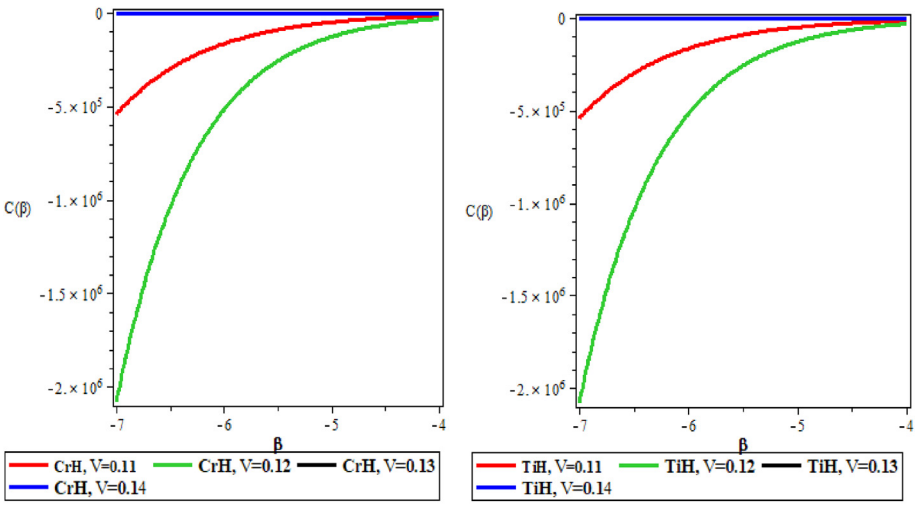

(a) (b)

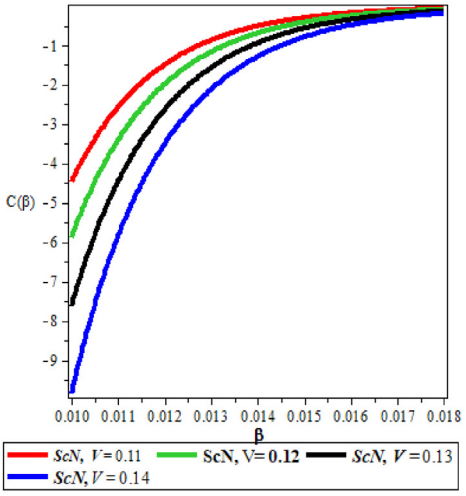

(c)

Figure 9. Variation of C(β) against β for CrH (a), TiH (b) and ScN (c).

(c) Vibrational entropy

$$S(\beta)=k\ln Z(\beta)-k\beta\frac{\ln Z(\beta)}{\partial\beta^2}=k\ln\left[\frac{e^{-\beta\upsilon_1+2\beta\upsilon_1-\chi_2}\sqrt{\pi}[1+\chi_4+e^{2\chi_2}(\chi_5+1)]}{4\sqrt{-\beta\upsilon_2}}\right]$$
$$-K\beta\left\{\frac{\left[1+\chi_4+e^{2\chi_2}(\chi_5-1)-2\beta\left(1+\chi_4+e^{2\chi_2}(\chi_5+1)\right)\omega_0+\left[\frac{4\sqrt{-\beta\upsilon_2}\left(\sqrt{\pi}\beta(e^{2\chi_2}\chi_5-e^{2\chi_2}-\chi_4-1)\upsilon_2\upsilon_3^2-e^{\chi_2+\omega_2\omega_6}\right)}{\sqrt{\pi}\omega_6}\right]\right]}{2\beta[1+\chi_4+e^{2\chi_2}(\chi_5-1)]}\right\} \quad (56)$$

Eq. (56) is a vibrational entropy.

(d) Vibrational free energy

$$F(\beta)=-\frac{1}{\beta}\ln Z(\beta)=-\frac{e^{\beta\omega_0}\ln\sqrt{\pi}[e^{\chi_3}(\chi_4+1)+e^{\chi_2}(\chi_5-1)]}{4\beta\sqrt{-\beta\upsilon_2}} \quad (57)$$

Eq. (57) is a vibrational free energy

4. Results and discussion

Table 1 shows the standard spectroscopic parameters for all the diatomic molecules used in this work. Tables 2 and 3 are the numerical bound state energies computed using Eq. (26), the spectroscopic constants of Table 1 and the arbitrary constants $(a, a_1, ..a_6 = 1.0)$ and $(a, a_1, ..a_6 = -1.0)$ for CrH, TiH and ScN molecules respectively. From Tables 2 and 3, the numerical bound state solutions of these molecules decreases with an increase in quantum state but increases with an increase in the angular momentum quantum state. Table 4 are the numerical solutions of Hellmann potential and Coulomb potential as special cases of the potential in the present work. The results of the special cases in Table 4 were also compared with an existing literature. The numerical solutions as reported in this table are in excellent agreement with the reports of other researchers.

Figure 1 (a) shows the potential for the present study. Figure 1(b) shows the approximation scheme. Figure 2 is the variation of bound state energy spectral with screening parameter λ and dissociation energy D_e (is presented). The variation of spectral in Figure 2 shows unique quantisation of different energy level. Figures 3(a-d) shows the wave function

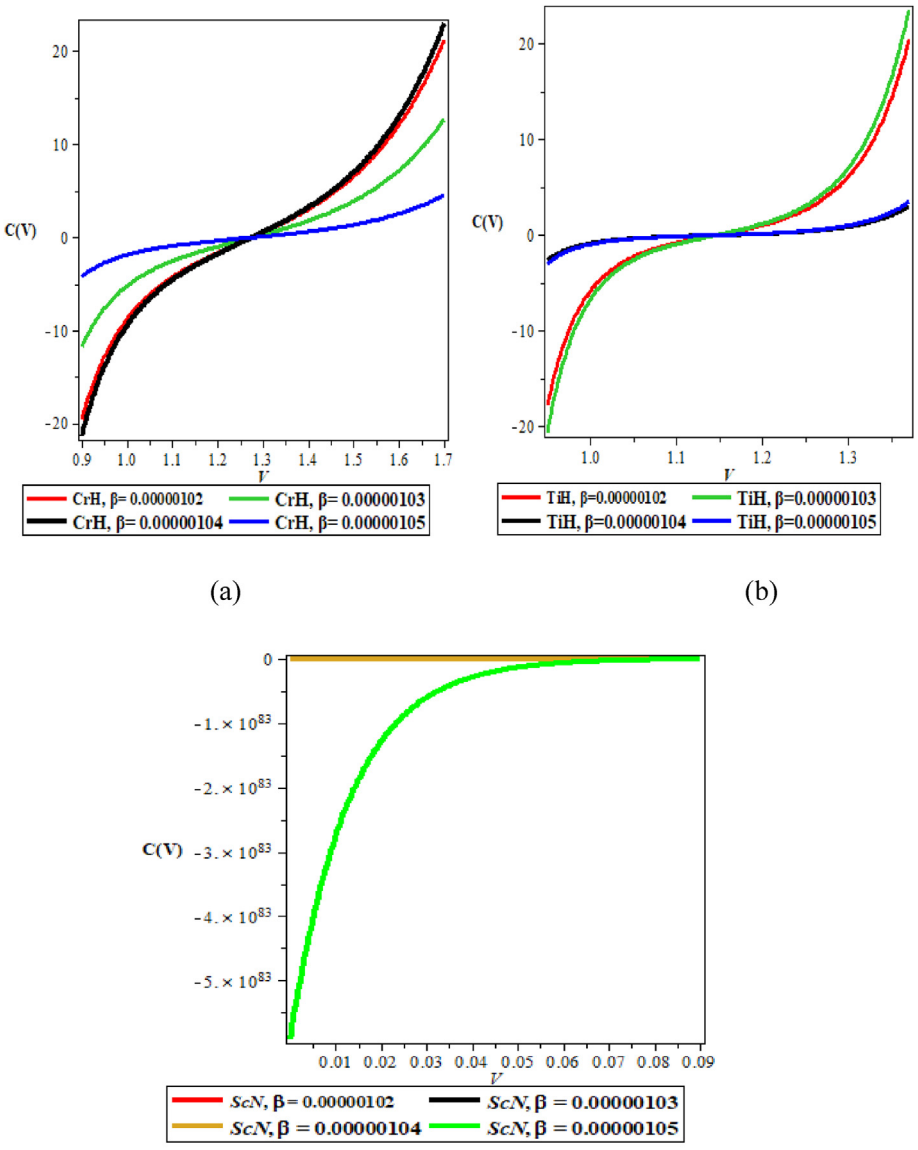

Figure 10. Variation of C(λ) against λ for CrH (a), TiH (b) and ScN (c).

and probability density for orbital angular quantum number $l = 0$ and $l = 1$ respectively. While Figures 4 (a-d) are the wave function plots and probability density plots for orbital angular quantum number $l = 2$ and $l = 3$ respectively. Both Figures 3(a-d) and 4(a-d) reproduces similar trend as reported in other literatures.

In Figure 5 and Figure 6, we examined the how the vibrational partition function varies with the temperature parameter and maximum quantum state for CrH, TiH and ScN. In Figure 5, the partition function and the temperature varies inversely with each other for the three diatomic molecular systems. At absolute zero, the partition function at various maximum quantum state tends to converged but diverged as the temperature decreases. In Figure 6, the partition function increases as the maximum quantum state increases for TiH and ScN. However, for CrH, the partition function decreases for $\beta = 0.00000102$, 0.00000103 and 0.00000104 but increases for $\beta = 0.00000105$ as the maximum quantum state increases. The behaviour of partition function against V for TiH and ScN are similar while that of CrH differes.

The variation of the vibrational mean energy against the temperature parameter and maximum quantum state respectively for CrH, TiH and ScN are shown in Figures 7 and 8. In Figure 7, the vibrational mean energy decreases monotonically as the temperature of the system decreases gradually for all the molecules. The vibrational mean energy at various V are the same for three molecules at all values of β. Although, the mean energy for the three molecules exhibit the same features but that of the ScN has lower values compared to CrH and TiH. In Figure 8, the vibrational mean energy increases as the maximum quantum state increases for TiH. However, for CrH, the vibrational mean energy decreases for the first $\beta = 0.00000102$, 0.00000103 and 0.00000104 and the mean energy are found to be greater than zero but for $\beta = 0.00000105$, the mean energy increases as V increases. The mean for the last value of β

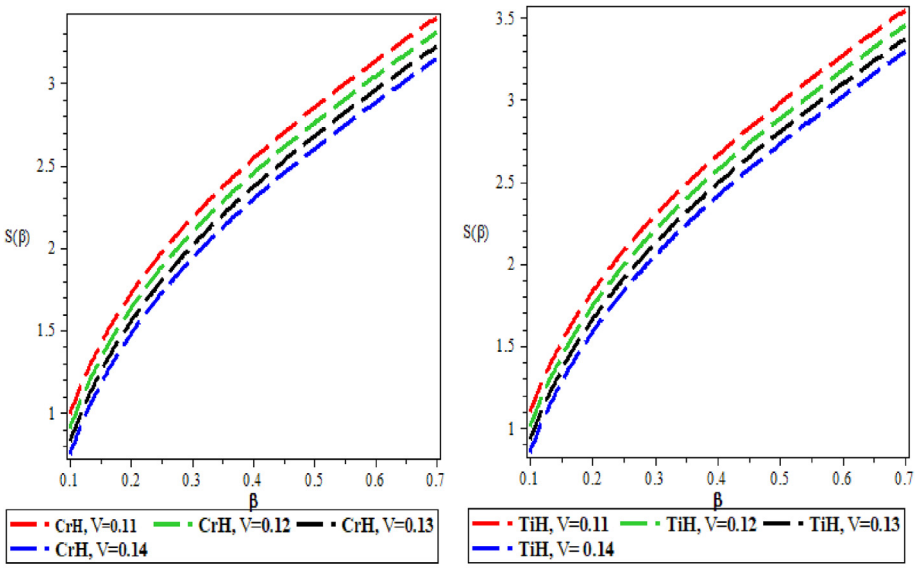

(a) (b)

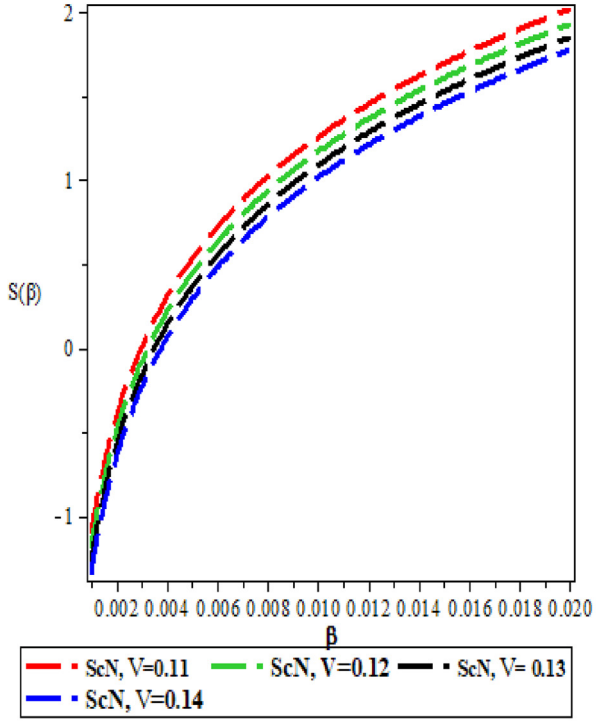

(c)

Figure 11. Variation S(β) against β for CrH (a), TiH (b) and ScN (c).

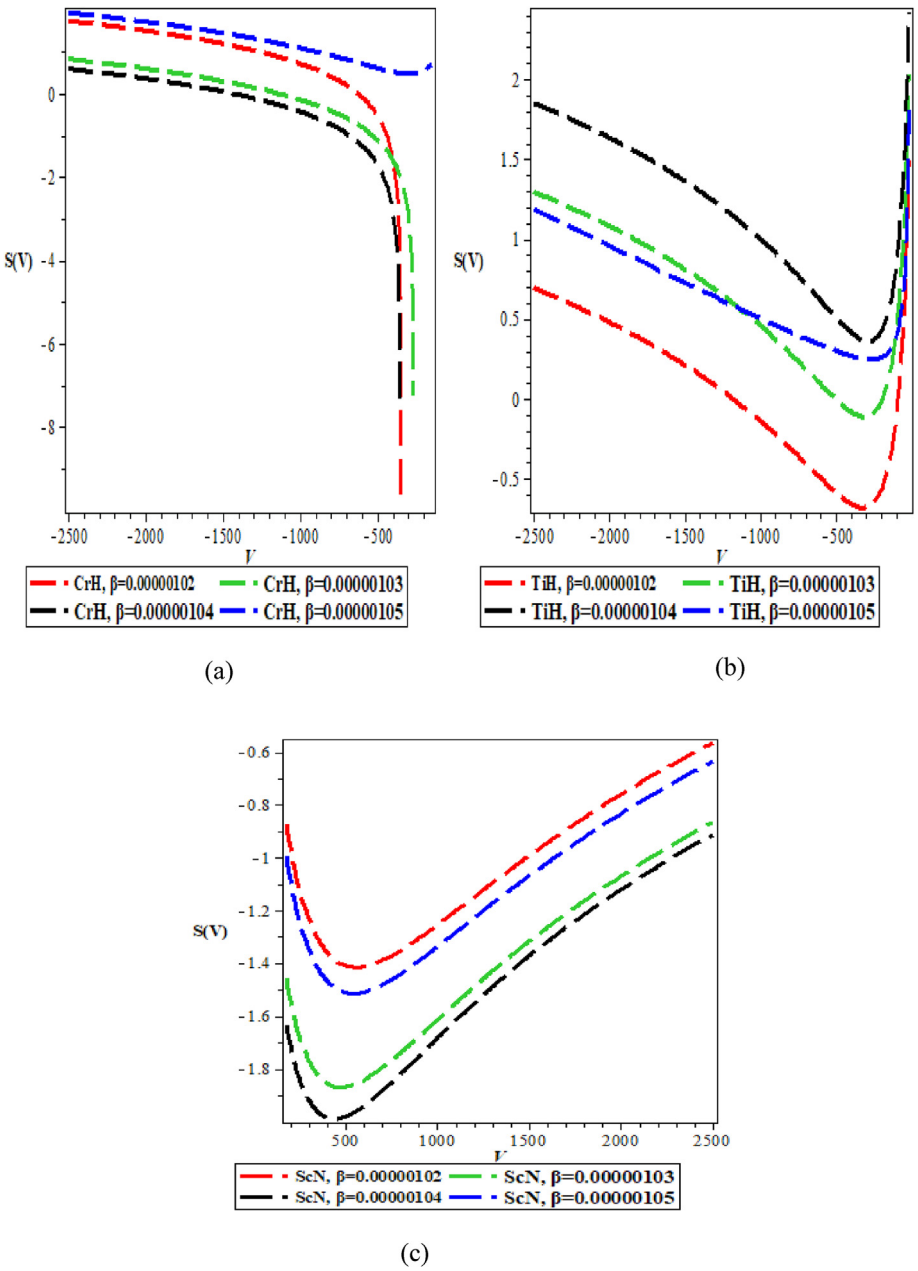

Figure 12. Variation S(λ) entropy against λ for CrH (a), TiH (b) and ScN (c).

even when it increases is seen to be less than zero. The behaviour of the mean energy against V for ScN is opposite to that of the CrH.

The variation of the vibrational specific heat against the temperature parameter and maximum quantum state for CrH, TiH and ScN are shown in Figures 9 and 10 respectively. In Figure 9, the specific heat capacity rises significantly as the temperature parameter increases for all the molecules. The specific heat capacity at different values of V tends to converge as the specific heat capacity is almost zero. In Figure 10, though the specific heat capacity rises as the maximum quantum state increases for all molecules, but the variation in CrH and TiH are the same while that of ScN differs. In Figures 10 (a) and (b), the specific heat capacity for various β converges when the specific heat capacity is zero after which they diverged as the rise significantly.

In Figures 11 and 12, we plotted the vibrational entropy against the temperature parameter and maximum quantum state for CrH, TiH and ScN. The vibrational entropy increases while the temperature parameter increases for the three molecules considered in this work. The vibrational entropy for various maximum quantum state diverged as they increase from zero. In Figure 12, the vibrational entropy for TiN and ScN decreases and have a turning point as the maximum quantum state increases steadily. The turning point for the two molecules are not very far from each other. For CrH, the vibrational entropy decreases as the maximum quantum state increases.

The variation of the vibrational free energy against the temperature parameter and the maximum quantum state for CrH, TiH and ScN are shown in Figures 13 and 14 respectively. The vibrational free energy for

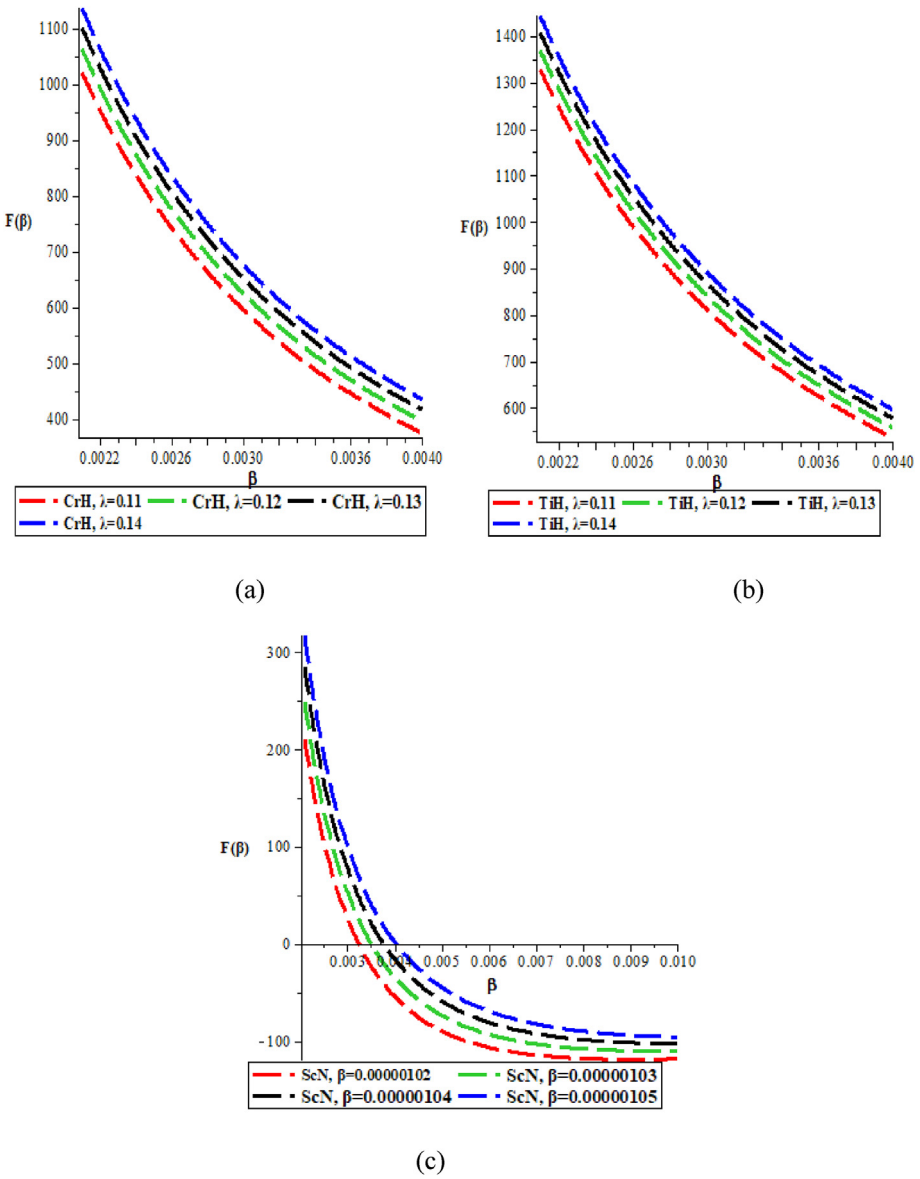

Figure 13. Variation F(β) against β for CrH (a), TiH (b) and ScN (c).

all maximum quantum state decreases monotonically as the temperature parameter increases gradually for the three molecules in Figure 13. However, the vibrational free energy for various V for ScN converged when the β is zero and diverged as β gradually increases. This particular feature is not observed in CrH and TiH. In Figure 14, CrH and ScN have the same variation while that of TiH differs. The vibrational free energy increases as V increases for CrH and ScN, though the increase terms to be insignificant for V ranges from 0 to about 3 and a sharp increase is noticed but the vibrational free energy of TiH decreases as V increases for some values before it begins to have a turning point. The thermal properties are useful in different scientific fields e.g. regulation of heat content.

5. Conclusion

In this research work we calculated an approximate bound state solutions of four parameter Morse potential using supersymmetric quantum mechanics approach. The energy eigen equation is presented in a closed form and extended to study partition function and other thermodynamic properties for three diatomic molecules using standard spectroscopic constants. The proposed potential reduces to Improved Rosen Morse, Hellmann, Yukawa and Coulomb potential as special cases. The numerical bound state solutions obtained for some of the special cases are in excellent agreement with an existing literature. The normalised wave function and probability density plots were obtained for various quantum

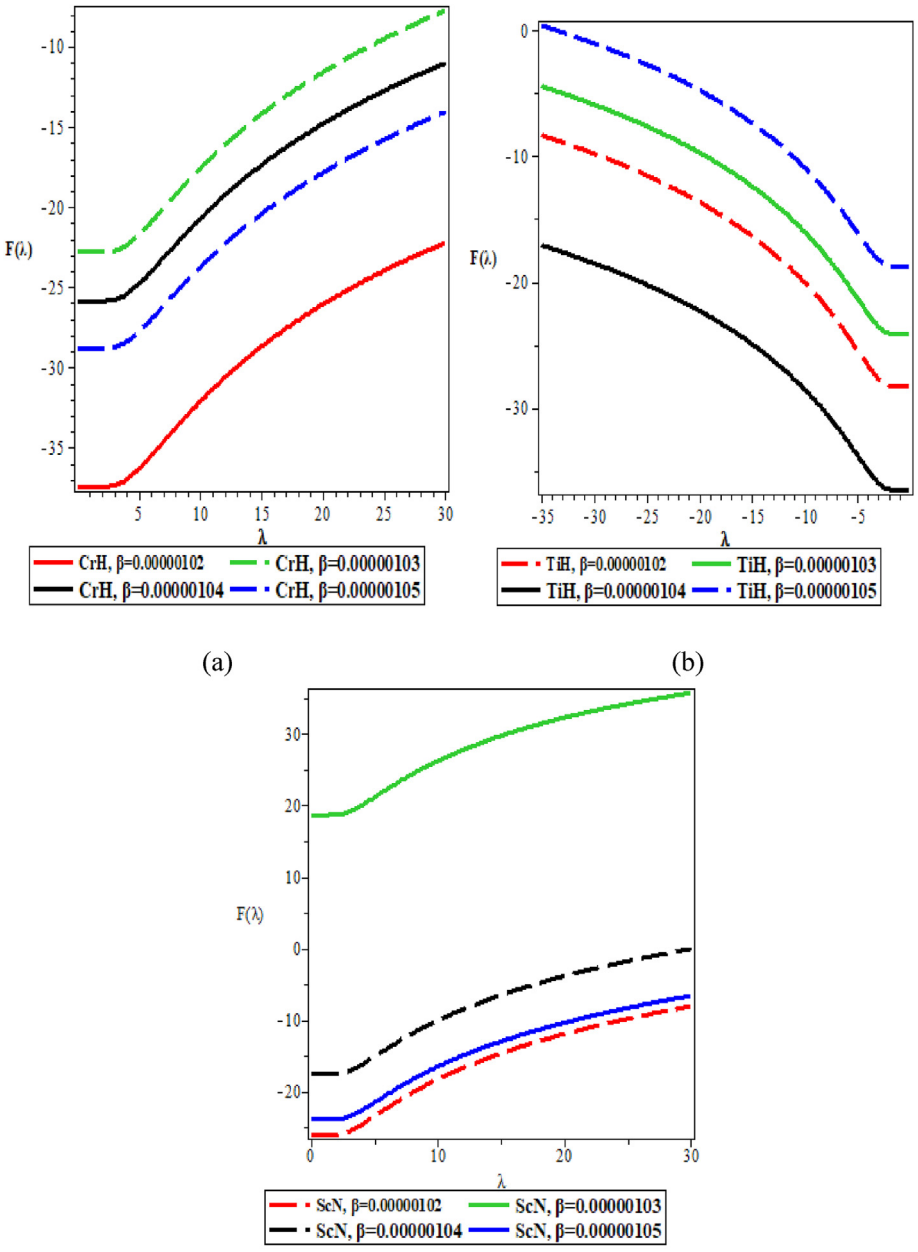

Figure 14. Variation F(λ) against λ for CrH (a), TiH (b) and ScN (c).

state and orbital angular quantum number. The thermal properties for the three molecules studied in some cases showed the same characteristics while in some areas, their thermal properties exhibit different features. The results obtained are applicable in Molecular Physics especially in the field of spectroscopy.

Declarations

Author contribution statement

C.A. Onate: Conceived and designed the experiments; Analyzed and interpreted the data; Wrote the paper.

I.B. Okon: Conceived and designed the experiments; Performed the experiments; Wrote the paper.

E. Omugbe, A.D. Antia: Performed the experiments; Wrote the paper.

M.C. Onyeaju: Analyzed and interpreted the data; Wrote the paper.

J.P. Araujo, Chen Wen-Li: Contributed reagents, materials, analysis tools or data; Wrote the paper.

Funding statement

This research did not receive any specific grant from funding agencies in the public, commercial, or not-for-profit sectors.

Data availability statement

No data was used for the research described in the article.

Declaration of interest's statement

The authors declare no conflict of interest.

Additional information

No additional information is available for this paper.

References

[1] C.A. Onate, T.A. Akanbi, I.B. Okon, Ro-vibrational energies of Cesium dimer and Lithium dimer with molecular attractive potential, Sci. Rep. 11 (2021) 6198.

[2] I.B. Okon, A.D. Antia, L.E. Akpabio, B.U. Archibong, Expectation values of some diatomic molecules with Deng-fan potential using Hellmann- Feynman Theorem, J. Appl. Phys. Sci. Int. 10 (2018) 247.

[3] B.J. Falaye, K.J. Oyewumi, S.M. Ikhdair, M. Hamzavi, Eigensolution techniques, their applications and Fisher's information entropy of the Tietz–Wei diatomic molecular model, Phys. Scripta 89 (2014), 115204.

[4] X.T. Hu, J.Y. Liu, C.S. Jia, The $3^3\sum^+_g$ state of Cs_2 molecule, Comput. Theor. Chem. 1019 (2013) 137–140.

[5] R. Horchani, N. Al-Kindi, H. Jelassi, Ro-vibrational energies of caesium molecules with the tietz–Hua oscillator, Mol. Phys. 120 (2020), e1812746.

[6] C.A. Onate, M.C. Onyeaju, E.E. Ituen, A.N. Ikot, O. Ebomwonyi, J.O. Okoro, Eigensolutions, Shannon entropy and information energy for modified Tietz–Hua potential, Indian J. Phys. 92 (2018) 487–493.

[7] C.A. Onate, M.C. Onyeaju, E. Omugbe, I.B. Okon, O.E. Osafile, Bound state solutions and thermal properties of modified Tietz-Hua potential, Sci. Rep. 11 (2021) 2129.

[8] A.M. Desai, N. Mesquita, V. Fernandes, A new modified Morse potential energy function for diatomic molecules, Phys. Scripta 95 (2020), 085401.

[9] A.N. Ikot, W. Azogor, U.S. Okorie, F.E. Bazuaye, M.C. Onyeaju, C.A. Onate, E.O. Chukwuocha, Exact and Poisson summation thermodynamic properties for diatomic molecules with Tietz potential, Indian J. Phys. 93 (2019) 1171–1179.

[10] I.B. Okon, O.O. Popoola, E. Omugbe, A.D. Antia, C.N. Isonguyo, E.E. Ituen, Thermodynamic properties and bound state solutions of Schrodinger equation with Mobius square plus screened –kratzer potential using Nikiforov-Uvarov method, Comput. Theor. Chem. 1196 (2021), 113132.

[11] E. Omugbe, O.E. Osafile, M.C. Onyeaju, I.B. Okon, C.A. Onate, The unified treatment on the non-relativistic bound state solutions, thermodynamic properties and expectation values of exponential-type potentials, Can. J. Phys. 99 (2021) 521–532.

[12] E. Omugbe, O.E. Osafile, I.B. Okon, E.A. Enaibe, M.C. Onyeaju, Bound state solutions, Fisher Information measures, expectation values and transmission coefficient of the Varshni potential, Mol. Phys. 119 (2021), e1909163.

[13] Y.P. Varshni, Comparative study of the potential energy function for diatomic molecules, Rev. Mod. Phys. 29 (1957) 664.

[14] C.N. Isonguyo, I.B. Okon, A.N. Ikot, H. Hassanabadi, Solution of klein-gordon equation for some diatomic molecules with new generalised morse-like potential using SUSYQM, Bull. Kor. Chem. Soc. 35 (2014), 123443.

[15] E. Omugbe, O.E. Osafile, I.B. Okon, M.C. Onyeaju, Energy Spectrum and the properties of the Schiöberg potential using the WKB approximation approach, Mol. Phys. 119 (2020), e1818860.

[16] R.N.C. Filho, G. Alencar, B.S. Skagerstam, J.S. Andrade, Morse potential derived from first principle, Europhys. Lett. 101 (2013), 10009.

[19] Y. Gao, E.W. Prohofsk, A modified self -consistent phonon theory of hydrogen bond melting, J. Chem. Phys. 80 (1984) 2242.

[20] Y. Gao, K.V. Devi-Prasad, E.W. Prohofsk, A self –consistent microscopic theory of hydrogen bond melting with application to poly (dG). poly (dC), J. Chem. Phys. 80 (1984) 6291.

[21] M. Peyrard, A.R. Bishop, Statistical Mechanics of a nonlinear model for DNA denaturation, Phys. Rev. Lett. 62 (1989) 2755.

[22] N. Theodorakopoulos, T. Dauxois, M. Peyrard, Order of the phase transition in models of DNA thermal denaturation, Phys. Rev. Lett. 85 (2000) 6.

[23] A.M. Theaban, K.S. Wadi, Morse potential rotation effect and effective potential for Li_2^7 molecule, J. Phys.: Conf. Ser. 1178 (2019), 012030.

[24] J.J. Pena, A. Menendez, J. Garcia-Ravelo, J. Morales, Mie-Type potential from a class of multi parameter-exponential type potential: bound State solutions in D-dimension, J. Phys. Conf. 63 (2015), 012025.

[25] A.I. Ahmadov, C. Aydin, O. Uzun, Bound state solution of the Schrödinger equation at finite temperature, J. Phys.: Conf. Ser. 1194 (2019), 012001.

[26] A.I. Ahmadov, K.H. Abasova, M. Sh, Orucova. Bound State Solution Schrödinger Equation for Extended Cornell Potential at Finite Temperature, Adv High Energy Phys. (2012) (2021). Article ID 1861946.

[27] Y.-J. Shi, G.-H. Sun, F. Tahir, A.I. Ahmadov, B. He, S.-H. Dong, Quantum information measures of infinite spherical well, Mod. Phys. Lett. A 33 (2018) 1850088.

[28] M. Eshghi, H. Mehraban, Study of a 2D charged particle confined by a magnetic and AB flux fields under the radial scalar power potential, Eur. Phys. J. Plus 132 (2017) 121.

[29] U.S. Okorie, A.N. Ikot, E.O. Chukwuocha, G.J. Rampho, Thermodynamic properties of improved deformed exponential –type potential (IDEP) for some diatomic molecules, Results Phys. 17 (2020), 103078.

[30] S. Meyur, S. Debnath, Eigen spectra for Woods-Saxon plus Rosen-Morse potential, Lat. Am. J. Phys. Educ. 4 (2010) 587–597.

[31] I. Nasser, M.S. Abdelmonem, H. Bahlouli, A.D. Alhaidari, The rotating Morse potential model for diatomic molecules in the tridiagonal J-matrix representation: I. Bound states, J. Phys. B Atom. Mol. Opt. Phys. 40 (2007) 4245–4257.

[32] T. Barakat, K. Abodayeh, O.M. Al-Dossary, Exact solutions for vibrational levels of the Morse potential via the asymptotic iteration method, Czech. J. Phys. 56 (2006) 538–590.

[33] M. Hamzavi, K.E. Thylwe, A.A. Rajabi, Approximate bound states solution of the Hellmann potential, Commun. Theor. Phys. 66 (2013) 1–8.

[34] S.A. Moghadam, M. Eshghi, H. Mehraban, Solution of the Dirac equation for pseudoharmonic oscillatory ring-shaped potential by the supersymmetric quantum mechanics, Phys. Scripta 89 (2014), 095202.

[35] M. Eshghia, H. Mehraban, M. Ghafoori, Non-relativistic Eigen spectra with *q*-deformed physical potentials by using the SUSY approach, Math. Methods Appl. Sci. 40 (2017) 1003–1018.

[36] M. Eshghi, H. Mehraban, S.M. Ikhdair, The relativistic bound states of a non-central potential, Pramana - J. Phys. 88 (2017) 73.

[37] G.-F. Wei, S.–H. Dong, A novel algebraic approach to spin symmetry for Dirac equation with scalar and vsctor Second Pöschl-Teller potentials, Eur. Phys. J. A 43 (2010) 185–190.

[38] C.S. Jia, Y.F. Diao, X.-J. Liu, P.-Q. Wang, J.-Yi. Liu, Equivalence of the Wei potential model and Tietz potential model for diatomic molecules, J. Chem. Phys. 137 (2012), 014101.

[39] M. Hamzavi, K.E. Thylwe, A.A. Rajabi, Approximate bound state solution of Hellmann potential, Commun. Theor. Phys. 60 (2013) 1–3.

[40] S.M. Ikhdair, R. Sever, A perturbartive treatment for the bound states of the Hellmann potential, J. Mol. Struct. Theochem. 809 (2007) 103–113.